

Inter-grain tunneling in the half-metallic double-perovskites $\text{Sr}_2\text{BB}'\text{O}_6$ (BB'– FeMo, FeRe, CrMo, CrW, CrRe)

B. Fisher,* J. Genossar, K. B. Chashka, L. Patlagan, and G. M. Reisner

Physics Department, Technion, Haifa 32000, Israel.

(Dated: September 5, 2018)

Abstract

The zero-field conductivities (σ) of the polycrystalline title materials, are governed by inter-grain transport. In the majority of cases their $\sigma(T)$ can be described by the "fluctuation induced tunneling" model. Analysis of the results in terms of this model reveals two remarkable features: 1. For *all* $\text{Sr}_2\text{FeMoO}_6$ samples of various microstructures, the tunneling constant (barrier width \times inverse decay-length of the wave-function) is ~ 2 , indicating the existence of an intrinsic insulating boundary layer with a well defined electronic (and magnetic) structure. 2. The tunneling constant for *all* cold-pressed samples decreases linearly with increasing magnetic-moment/formula-unit.

PACS numbers: 72.25.Ba 72.25.Hg 73.20.At 73.40.Gk

Half-metallic ordered double-perovskites with fully polarized conduction bands and Curie temperatures (T_c) above room temperature (RT) are of interest for devices which depend on spin polarized transport. Therefore their magnetic, electronic and in particular their magneto-resistive properties¹ have been investigated intensively over the past two decades. The grain boundaries in these materials act in most cases as tunnel barriers. The early theories of inter-grain tunneling magneto-resistance addressed the problem of tunneling through a non-magnetic barrier separating two ferromagnetic grains (including vacuum).²⁻⁴ These theories could not explain inter-grain magneto-resistance in half metals. In Ref. 5 the magneto-resistive behaviour of $(\text{BaSr})_2\text{FeMoO}_6$ was explained in terms of tunneling between two correlated spin glass-like surfaces separated by a thin insulating layer. In Ref. 6 it was suggested that the pinned ferromagnetic spins at the core/skin interface should be taken as being solely responsible for the tunneling magneto-resistance in half-metallic double-perovskites. A spin-glass-like surface layer surrounding each soft ferromagnetic (FM) grain of $\text{Sr}_2\text{FeMoO}_6$ has been detected also in Ref. 7 by careful ac susceptibility measurements on a highly ordered polycrystalline sample; these measurements were able to separate the barrier layer signal from the bulk. The presence of an intrinsic insulating boundary layer around FM grains of $(\text{LaSr})\text{MnO}_3$ (LSMO), with magnetic properties different from those of the bulk, has been recently revealed by means of x-ray linear dichroism and transport measurements.⁸ This phase, about 2 unit cells thick, is held responsible for the observed depressed magneto-transport properties in manganite based magnetic tunneling junctions.

Unlike the difficulty in separating the magnetic properties of the layers from those of the bulk,⁷ it is relatively easy to study the electronic properties of the grain skin layers when the electronic transport is dominated by inter-grain tunneling as is the case in most of the polycrystalline samples of the title materials. In this report we focus on the zero-field conductivity of various samples of the five title compounds; this comparative study revealed some important features of the grain-boundaries of these half metals.

Table I shows the five title double-perovskites (with abbreviations), their ionic configuration, nominal (ideal) saturation magnetization (M_i) and T_c . While their bulk is metallic, as confirmed by their metallic-like thermopower,¹⁰ the zero-field conductivities ($\sigma(T)$) of polycrystalline samples are non-metallic (the conductivity increases with increasing T). Metallic-like resistivity was found in a single crystal of SFMO.¹¹ The inter-grain tunneling conductivity depends strongly on preparation conditions and often exhibits unusual T-

dependence. The most remarkable behaviors are the linear-in- T conductivities from liquid He temperatures up to RT, for *all* our sintered and granular samples of SFMO, irrespective of preparation conditions, for some samples of SFRO and of SCMO, and the linear-in- T^2 conductivity over the same range of T , for some samples of SCMO.¹² The temperature dependence of the conductivity for all our samples, except for porous SCRO, can be derived from the "fluctuation induced tunneling" (FIT) model.¹³ This model applies to metallic grains embedded in an insulating medium. Tunneling occurs across small gaps (width w and area A) between large metallic grains; the small gaps are subject to large thermal fluctuations of the voltage.

$\sigma(T)$ predicted by this model is:

$$\sigma = \sigma_o \exp\left(-\frac{T_1}{T_o + T}\right) = \sigma(0) \exp\left(\frac{T_1 T}{T_o(T_o + T)}\right) \quad (1)$$

where $k_B T_1 = (2/\pi)(A/w)(V_o/e)^2$ is the electrostatic energy within a parabolic potential barrier of width w and height V_o of a junction of area A ; $T_1/T_o = \pi\chi w/2$ is the tunneling constant where $\chi = \sqrt{2mV_o/\hbar^2}$, σ_o is a pre-exponent that may be regarded as independent of temperature and $\sigma(0) = \sigma_o \exp(-T_1/T_o)$. The FIT equation for $\sigma(T)$ is an extension of the formula derived for a single junction to a network of fluctuating tunneling junctions.¹³ For $T \ll T_o$, Eq. (1) represents elastic tunneling and for $T \gg T_o$ - activated conductivity with activation energy $k_B T_1$. The effect of the thermal fluctuations is to reduce the barrier's height and width; for $T = T_o$ the effective tunneling constant is half its value at $T = 0$. This equation includes the rare and interesting cases mentioned above for specific ranges of the parameter T_1/T_o and of T/T_o . In Ref. 12 we showed that for $T_1/T_o < 3$ a linear function of T fits $\sigma(T)$ over a T/T_o range that increases with T_1/T_o . The correlation parameter of the linear fit to Eq. (1) for $T_1/T_o \lesssim 3$ and $T/T_o \leq 1.1$ is $R^2 = 0.9999$. In this range, $\sigma(T)$ varies up to a factor of 5, in good agreement with our findings (see Fig. 4 in Ref. 12). We showed also that $(\sigma(T) - \sigma(0)) \propto T^2$ ($R^2 = 0.9999$), for a narrow range of T_1/T_o around 8 and T/T_o up to ~ 1.8 . Within this range $\sigma(T)$ may vary by more than two orders of magnitude, again in good agreement with our findings (see Fig. 3 in Ref. 12).

All SFMO samples exhibit linear $\sigma(T)$. In other compounds conductivity linear-in- T or linear-in- T^2 (over a wide temperature range) are special cases. However, except for SCRO, $\sigma(T)$ for all sintered samples obeys the FIT model with parameters within a wide range that depend on the preparation conditions. Our sintered SCRO samples were porous

and their conductivity over an unprecedentedly wide range of T was of Berthelot-type ($\ln(\sigma(T)/\sigma(0)) = T/T_B$ where T_B is a constant of the order of a few tens of K).¹⁴ This behavior can be derived from Tredgold's "vibrating barrier tunneling" model.¹⁵ Eq. (1) can be reduced to a Berthelot-type formula for $T_1/T_o \gg 1$ and $T/T_o \ll 1$ with $T_B = T_o^2/T_1$ but then the values of the fitting parameters to our data become non-physical. Interestingly, $\sigma(T)$ for cold-pressed (c.p.) SCRO obeys the FIT model with reasonable parameters (see below).

The FIT model has been extended to electric-field dependent conductivities. The nonlinear I-V characteristics measured on some SFMO samples (using pulsed currents in order to avoid Joule heating) are consistent with the extended FIT model, at least qualitatively.¹⁶

The FIT model does not address magnetic interactions. Since it was applied successfully to at least three groups of magnetic materials (our title materials, CrO_2 and its composites^{17,18} and Co-based nanocomposites¹⁹), it may be assumed that the influence of the magnetic interactions is on the nature of the tunneling barrier and on the pre-exponent. Since M_i of our samples varies between 1 and 4, we attempted to detect correlations between the tunneling parameters of the exponent of Eq. (1) and M_i .

Table II contains the fitting parameters of Eq. (1) to the experimental $\sigma(T)$: $\sigma(0)$, T_1 , T_o and T_1/T_o , for our samples of $\text{Sr}_2\text{BB}'\text{O}_6$. The labels of the five groups of samples are followed by the sources of the data (the relevant references to our previous publications and Figs. 1 and 2 shown here), M_i and fitting parameters. Only two parameters in the exponent are independent but for convenience all three are shown (T_1 , T_o and T_1/T_o). We also show the fitted parameters for a cold-pressed $\text{Sr}_{1.5}\text{La}_{0.5}\text{FeMoO}_6$ (LSFMO). Additional plots of $\sigma(T)$ for SFMO are shown in Ref. 16; all are straight lines up to RT. The slopes of the plots for the cold-pressed samples are steeper than those for the sintered samples. The conductivities of the samples at $T=0$ ($\sigma(0)$) spread over many orders of magnitude, from 10^{-6} to 10^2 (Ωcm)⁻¹. The highest $\sigma(0)$ ($= 74.5(\Omega\text{cm})^{-1}$, for sample SFMO(N1)) is about 50 times lower than the metallic conductivity of an SFMO single crystal at $T=0$.¹¹

The upper curve in Fig. 1(a) shows $\sigma(T)$ of a sintered SFRO sample that underwent a short heat treatment at 500°C in Ar5%H₂. The maximum indicates mixed grain-boundary and metallic conductivity. A similar behavior is seen in Fig. 2 of Ref. 20 for an SFRO sample sintered in Ar atmosphere. Prolonged heat treatment of our sample in air at 400°C restored inter-grain tunneling and the $\sigma(T)$ plot straightened up (see lower curve in Fig.

1(a)). The solid line represents Eq. (1) fitted to the experimental data. Fig. 1(b) shows three more plots of $\sigma(T)$ for SFRO samples, including one for a c.p. sample. The data for the c.p. sample exhibit unusual behavior at high temperatures and Eq. (1) could be fitted to this line only up to 250 K.

Fig. 2 presents plots of $\sigma(T)$ for c.p. samples of SCWO and SCRO that were not included in the previous reports^{9,14} since at that time they did not seem relevant for the main issues of those papers.

The three parameters T_1 , T_o and T_1/T_o are plotted versus M_i in Fig. 3(a)- (c). While no correlations are seen in Figs. 3(a)-(b), Fig. 3(c) exhibits two remarkable features:

1. The data of T_1/T_o (the tunneling constant $\pi\chi w/2$) for SFMO fall between 2 and 3, irrespective of microstructure of the samples. Within the FIT model this corresponds to the remarkable linearity of $\sigma(T)$. The independence from microstructure hints at the presence of an intrinsic insulating boundary layer through which tunneling occurs, with well-defined electronic (and magnetic) structure.

2. The data of T_1/T_o for cold pressed samples (*i.e.* for bare boundaries) lie close to a straight line that extrapolates to zero near $M_i = 5$ which corresponds to the d-gap (see Table I). The possibility that such a simple analytical function fits the dependence of $\pi\chi w/2$ on M_i for this set of half-metallic c.p. samples requires further experimental and theoretical support.

Our analysis shows that the quality of the tunneling barriers in inter-grain conductivity depends on T_o . The higher T_o relative to RT, the closer is inter-grain tunneling to elastic tunneling. Table II and Fig. 3(b) show that, for only 3 samples out of 19, $T_o > 1000$ K, *i.e.* for two polycrystalline samples of SFMO (in Fig. 3(b) the two symbols coincide) and for one c.p. sample of SFRO. Note that for SFMO(N1) the ratio $\sigma(RT)/\sigma(0)$ is only 1.25. The wide spread of the FIT parameters implies a broad range of interactions governing magneto-resistance (magneto-conductance). Results in Ref. 21 show that for sintered SFMO samples the magneto-conductance is much higher than that for a c.p. sample at all temperatures. This requires a more systematic investigation.

-
- * Electronic address: phr06bf@physics.technion.ac.il
- ¹ D. Serrate, J. M. De Teresa and M R Ibarra, *J. Phys. Condens. Matter* **19**, 023201 (2007) and references therein.
- ² M. Julliere, *Phys. Lett.* **54A**, 225 (1975).
- ³ J. C. Slonczewski, *Phys. Rev. B* **39**, 6995 (1989).
- ⁴ J. Inoue and S. Maekawa, *Phys. Rev. B* **53**, R11927 (1996).
- ⁵ D. Serrate, J. M. De Teresa, P. A. Algarabel, M. R. Ibarra, and J. Galibert, *Phys. Rev. B* **71**, 104409 (2005).
- ⁶ S. Jana, S. Middey and S. Ray, *J. Phys. Condens. Matter* **22**, 346004 (2010).
- ⁷ S. Ray, S. Middey, S. Jana, A. Banerjee, P. Sanyal, R. Rawat, L. Gregoratti and D. D. Sarma, *EPL*, **94**, 47007 (2011).
- ⁸ S. Valencia, L. Pena, Z. Konstantinovic, Ll. Balcells, R. Galceran, D. Schmitz, F. Sandiumenge, M. Casanove and B. Martinez, cond-mat arXiv:1302.5293.
- ⁹ Sr_2CrWO_6 has been confused in the past with $\text{Sr}_3\text{Cr}_2\text{WO}_9$, which has a much higher T_c . Preparation of these two distinct compounds as single phases was reported in: B. Fisher, K. B. Chashka, L. Patlagan, and G. M. Reisner, *Phys. Rev. B* **71**, 104428 (2005).
- ¹⁰ B. Fisher, J. Genossar, K. B. Chashka, L. Patlagan and G. M. Reisner, *Curr. Appl. Phys.* **7**, 151 (2007).
- ¹¹ Y. Tomioka, T. Okuda, Y. Okimoto, R. Kumai, K. -I. Kobayashi and Y. Tokura, *Phys. Rev. B* **61**, 422 (2000).
- ¹² B. Fisher, J. Genossar, K. B. Chashka, L. Patlagan, and G. M. Reisner, *Solid State Commun.* **137**, 641 (2006) and references therein.
- ¹³ Ping Sheng, *Phys. Rev. B* **21**, 2180 (1980) and references therein.
- ¹⁴ B. Fisher, K. B. Chashka, L. Patlagan, and G. M. Reisner, *Phys. Rev. B* **70**, 205109 (2004).
- ¹⁵ R. H. Tredgold, *Proc. Phys. Soc. London* **80**, 807 (1962).
- ¹⁶ B. Fisher, K. B. Chashka, L. Patlagan, and G. M. Reisner, *Phys. Rev. B* **68**, 134420 (2003).
- ¹⁷ A. Bajpai and A. K. Nigam, *Phys. Rev. B* **75**, 064403 (2007).
- ¹⁸ Fan Yin-Bo, Zhang Cai-Ping, Du Xiao-Bo, Wen Ge-Hui, Ma Hong-An and Jia Xiao-Peng, *Chin. Phys. Lett.* **30**, 037502 (2013).

- ¹⁹ T. Wen and K. M. Krishnan, *J. Phys. D: Appl. Phys.* **44**, 393001 (2011).
- ²⁰ K.-I. Kobayashi, T. Kimura, Y. Tomioka, H. Sawada, K. Terakura and Y. Tokura, *Phys. Rev. B* **59**, 11159 (1999).
- ²¹ B. Fisher, K. B. Chashka, L. Patlagan and G. M. Reisner, *J. Magn. Magn. Mater.* **272-276**, 1790 (2004).

TABLE I: The five $\text{Sr}_2\text{BB}'\text{O}_6$ half-metals, their ionic configurations, nominal saturation magnetization per formula unit (M_i) and Curie temperature (T_c (K))

$\text{Sr}_2\text{BB}'\text{O}_6$	Ionic configuration	M_i ($\mu_B/\text{f.u.}$)	T_c (K)
$\text{Sr}_2\text{FeMoO}_6$ (SFMO)	$\text{Fe}^{3+} (3d^5)\text{Mo}^{5+}(4d^1)$	4	420
$\text{Sr}_2\text{FeReO}_6$ (SFRO)	$\text{Fe}^{3+} (3d^5)\text{Re}^{5+}(5d^2)$	3	400
$\text{Sr}_2\text{CrMoO}_6$ (SCMO)	$\text{Cr}^{3+} (3d^3)\text{Mo}^{5+}(4d^1)$	2	450
Sr_2CrWO_6 ⁹ (SCWO)	$\text{Cr}^{3+}(3d^3)\text{W}^{5+} (5d^1)$	2	390
$\text{Sr}_2\text{CrReO}_6$ (SCRO)	$\text{Cr}^{3+}(3d^3)\text{Re}^{5+}(5d^2)$	1	635

Figure Captions

TABLE II: Fitting parameters for Eq. (1), for various $\text{Sr}_2\text{BB}'\text{O}_6$ polycrystalline samples.

Sample	Data source	M_i ($\mu_B/\text{f.u.}$)	$\sigma(0)$ (Ωcm) $^{-1}$	$T_1(\text{K})$	$T_o(\text{K})$	T_1/T_o
SFMO(N1)	Fig. 2 in Ref. 16	4	74.5	5171	2478	2.09
SFMO(r)	Fig.4 in Ref. 12	4	33.8	6989	2551	2.74
SFMO(c.p.)	Fig. 2 in Ref. 12	4	0.72	1586	582	2.73
SFRO (Ox)	Fig. 1(a)	3	2.50	396	494	0.80
SFRO (S1)	Fig. 1(b)	3	3.88	1117	703	1.59
SFRO (S2)	Fig. 1(b)	3	13.0	276	397	0.70
SFRO (c.p.)	Fig. 1(b)	3	0.19	8111	1329	6.10
SCMO(A)	Fig. 2(a) in Ref. 12	2	1.02	712	263	2.71
SCMO(C)	Fig. 2(a) in Ref. 12	2	2.48	455	117	3.89
SCMO(E)	Fig. 2(a) in Ref. 12	2	6.1	390	130	3.00
SCMO(A+Ox)	Fig. 2(b) in Ref. 12	2	4.6×10^{-4}	1104	207	5.33
SCMO(D)	Fig. 2(b) in Ref. 12	2	0.31	1405	228	6.16
SCMO(B1)	Fig. 3 in Ref. 12	2	6.3×10^{-4}	1430	180	7.94
SCMO(B2)	Fig. 3 in Ref. 12	2	5.6×10^{-4}	1177	152	7.74
SCWO	Fig. 6(a) in Ref.9	2	0.045	260	118	2.20
SCWO	Fig. 6(a) in Ref.9	2	0.030	461	213	2.16
SCWO (c.p.)	Fig. 2	2	2×10^{-6}	1850	200	9.25
SCRO (c.p.)	Fig. 2	1	1.2×10^{-4}	4071	383	10.63
LSFMO (c.p.)	Fig. 4 in Ref. 12	3.5	0.47	941	298	3.16

r - reduced, c.p. - cold-pressed, Ox - oxidized

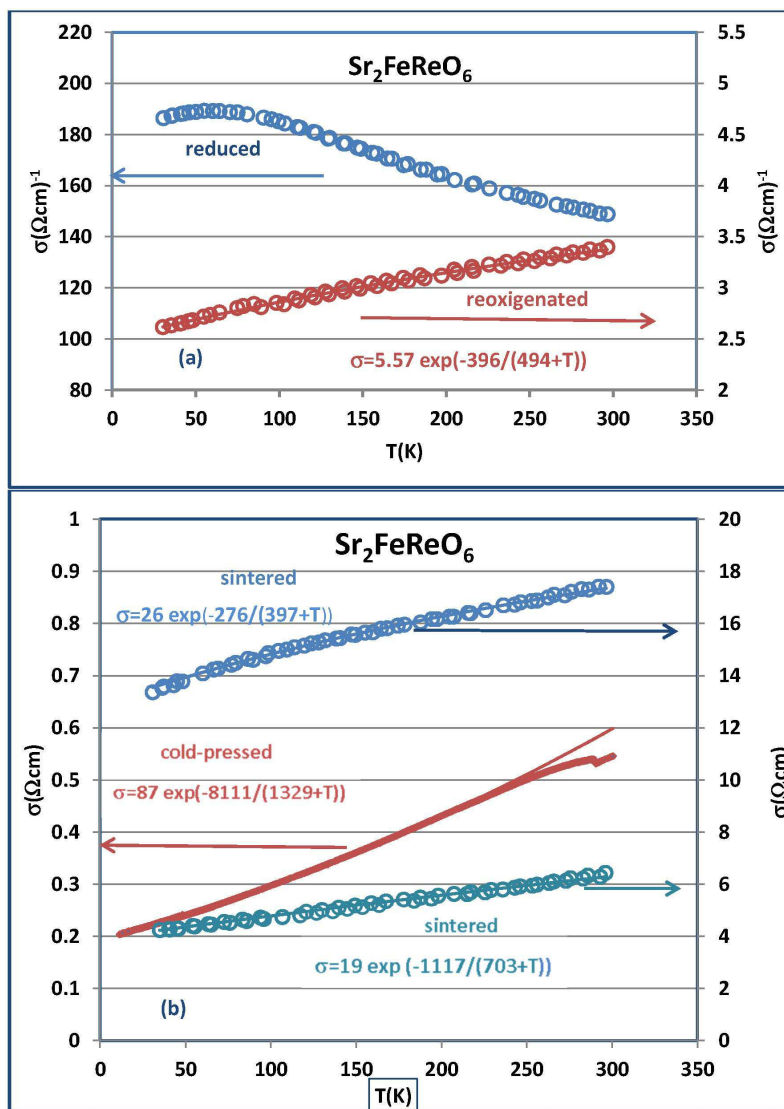


Fig. 1

FIG. 1: Conductivity versus temperature of (a) a sintered sample of $\text{Sr}_2\text{FeReO}_6$ heat treated at 500°C in a reducing atmosphere (upper curve) and later reoxygenated at 400°C (lower curve), and (b) two additional sintered samples and one cold pressed sample. Solid lines in (a) and (b) represent Eq. 1 fitted to experimental data.

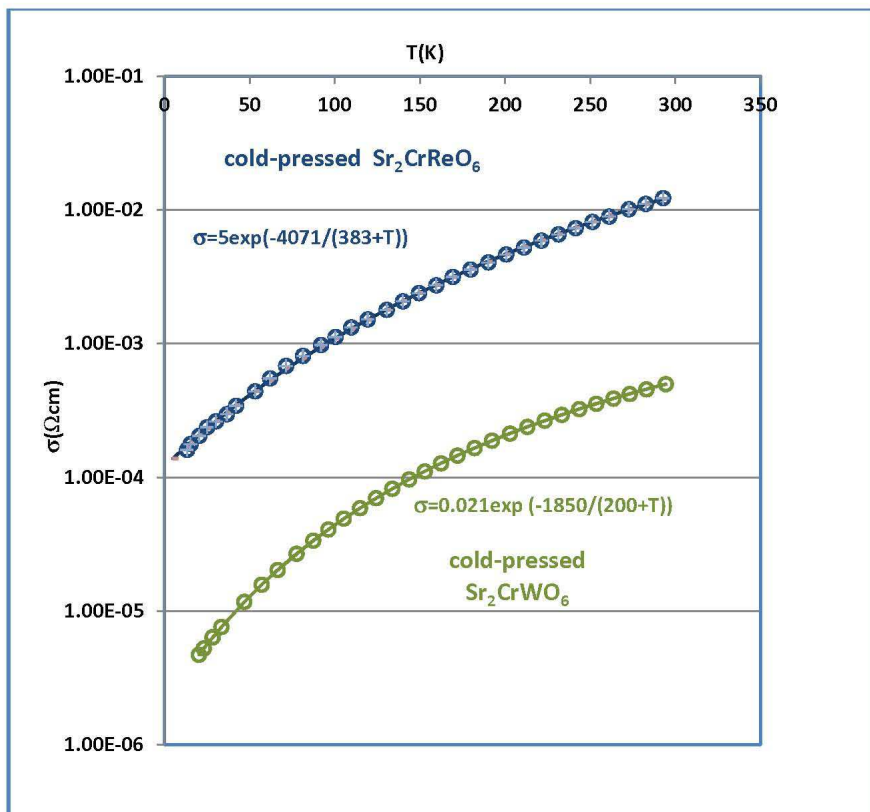


Fig. 2

FIG. 2: Conductivity versus T of cold-pressed samples of Sr_2CrWO_6 (lower curve) and $\text{Sr}_2\text{CrReO}_6$ (upper curve). Solid lines represent Eq. 1 fitted to experimental data.

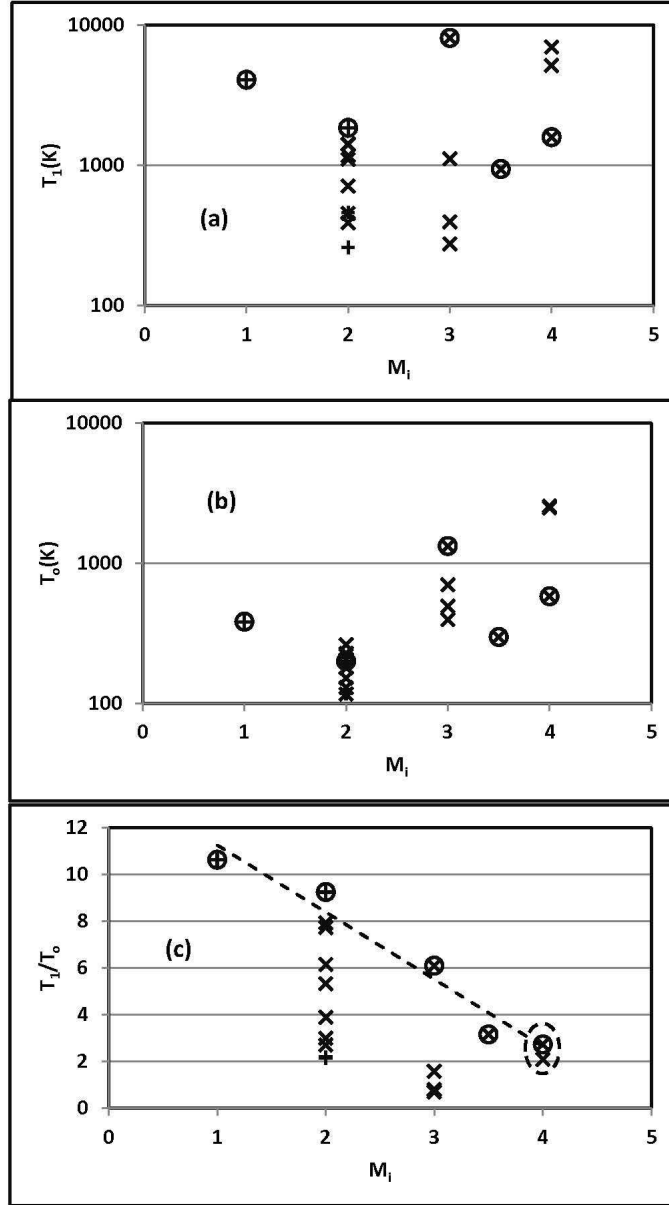


Fig.3

FIG. 3: Fitting parameters T_1 , T_0 and the tunneling constant - T_1/T_0 as function of M_i , the nominal saturation magnetization per formula unit. For $M_i = 2$ the symbol \times represents samples of SCMO and $+$ the samples of SCWO. Encircled symbols represent data for cold pressed samples. Note that for all SFMO samples, T_1/T_0 falls between 2 and 2.75 (within the range of linear $\sigma(T)$). The values of T_1/T_0 for the cold pressed samples increase almost linearly with M_i .